

**The Mauna Kea Observatories Near-Infrared Filter Set. II.
Specifications for a New $JHKLM'$ Filter Set for
Infrared Astronomy**

A. T. Tokunaga

Institute for Astronomy, University of Hawaii, Honolulu, HI 96822

`tokunaga@ifa.hawaii.edu`

D.A. Simons

*Gemini Observatory, Northern Operations Center, 670 N. A'ohoku Place,
Hilo, HI 96720*

`dsimons@gemini.edu`

and

W. D. Vacca

*Max-Planck-Institut für extraterrestrische Physik
Postfach 1312, D-85741 Garching, Germany*

`vacca@mpe.mpg.de`

ABSTRACT

We present a description of a new 1–5 μm filter set similar to the long-used $JHKLM$ filter set derived from that of Johnson. The new Mauna Kea Observatories Near-Infrared (MKO-NIR) filter set is designed to reduce background noise, improve photometric transformations from observatory to observatory, provide greater accuracy in extrapolating to zero air mass, and reduce the color dependence in the extinction coefficient in photometric reductions. We have also taken into account the requirements of adaptive optics in setting the flatness specification of the filters. A complete technical description is presented to facilitate the production of similar filters in the future.

Subject headings: infrared: general — instrumentation: photometers

1. Introduction

The rationale for a new set of infrared filters was presented by Simons & Tokunaga (2001; hereafter Paper I). The goals of the design of this new filter set are similar to those of Young, Milone, & Stagg (1994), namely to construct a filter set that minimized color terms in the transformations between photometric systems and that reduced the uncertainty in determining the absolute calibration of photometric systems. However, in contrast to the filters proposed by Young et al., the filters in this new set were also designed to maximize throughput, in addition to minimizing the effects of atmospheric absorption. The reduced dependence on atmospheric absorption also permits photometry to be less sensitive to water vapor variations and to the altitude of the observatory. Most importantly, the new filters permit extrapolation to zero air mass with small errors.

We required large-size, high-quality filters for several facility instruments for the Gemini and Subaru Telescopes. Since the cost of each filter is dominated by the technical difficulties of the coating process it is desirable to place as many substrates as possible into the coating chamber in order to reduce the cost per filter. Hence there is a strong economic driver to produce custom filters in a consortium production run. This has the added benefit that with more observatories involved there would be greater standardization among the observatories.

Although this filter set was designed for the Gemini and Subaru Telescopes, all of the optical/infrared observatories at Mauna Kea are presently using these filters (NASA Infrared Telescope Facility, United Kingdom Infrared Telescope, Canada-France-Hawaii Telescope, Keck, Gemini, Subaru). In addition, the filter set was discussed informally by the IAU Working Groups on IR Photometry and on Standard Stars at the 2000 General Assembly, and endorsed as the preferred “standard” near-infrared photometric system, to be known as the Mauna Kea Observatories Near-Infrared (MKO-NIR) photometric system.

In this paper we describe a set of filters that were fabricated according to the definitions presented in Paper I. We include a list of specifications so that similar filters can be produced in the future. It is our hope that if enough observatories adopt these filters, we will have greater uniformity among photometric systems, as well as reduced systematic errors when comparing observations from different observatories.

2. Filter Specifications

We present here the list of technical specifications that were required to be satisfied by the filter manufacturer. The center, cut-on, and cut-off wavelengths are given in Table 1, and they follow the filter definitions given in Paper I. The specifications for substrate flatness, parallelism of the filters, and use of a single substrate are required for use with adaptive optics systems.

1. *Out-of-band transmission:* $<10^{-4}$ out to $5.6\ \mu\text{m}$.

This specification is required for use with InSb detectors. For HgCdTe 2.5 μm cut-off detectors, the out-of-band blocking can be specified for wavelengths less than 3.0 μm instead of 5.6 μm . The desired blocking is better than 10^{-4} , but practical considerations such as cost and manufacturing difficulty make it impossible to go lower. In cases where blocking to this level or better is not possible, a separate blocking filter should be used. PK-50 is a suitable blocker for wavelengths less than 2.0 μm . For longer wavelengths, an interference blocking filter may be required for InSb detectors.

2. *Operating temperature: 65 K. Cold filter scans of witness samples to be provided, together with prediction of wavelength shift with temperature.*

The filters are expected to be used at 50–77 K, but the specified filter temperature was set at 65 K primarily because the Gemini and Subaru instruments were designed for use with InSb detectors and with cryogenic motors inside the cryostat. This requires cooling to 65 K to avoid excess thermal emission from the motors within the cryostat.

3. *Average transmission: $>80\%$ (goal $>90\%$).*
4. *Transmission between the 80% points to have a ripple of less than $\pm 5\%$.*
5. *Cut-on and cut-off: $\pm 0.5\%$ wavelength error.*
6. *Roll-off: $\%slope \leq 2.5\%$.*

The $\%slope = [\lambda(80\%) - \lambda(5\%)]/\lambda(5\%) \times 100$, where $\lambda(80\%)$ is the wavelength at 80% transmission and $\lambda(5\%)$ the wavelength at 5% transmission.

Ideally the filters should have a square “boxcar” shape for maximum throughput. The specifications on the average transmission, ripple, cut-on and cut-off uncertainty, and roll-off uncertainty are a compromise between the desired sharp edge, practical manufacturing specifications, and cost.

7. *Substrate surfaces parallel to $\leq 5''$.*
8. *Substrate flatness: $< 0.0138\lambda/(n - 1)$, where n is the index of refraction of the substrate (compatible with AO systems).*

For example, for $n = 1.5$, $\lambda = 2200$ nm, the substrate flatness should be < 61 nm. For $n = 3.4$, $\lambda = 2200$ nm, the substrate flatness should be < 13 nm.

This is a flatness specification, not a roughness specification. The Strehl ratio (SR) can be approximated as $SR \sim 1 - [(2\pi/\lambda)w]^2$, where w is the rms wavefront error (see Schroeder 1987). This expression is valid for a single reflective surface. For two surfaces in transmission, we have $SR \sim 1 - [(n - 1)(2\pi/\lambda)w\sqrt{2}]^2$, where n is the index of refraction of the substrate. For $SR = 0.985$, $w = 0.01378[\lambda/(n - 1)]$. Alternatively, one could specify $\lambda/10$ peak-to-valley at 0.63 μm , which is approximately $\lambda/40$ rms, or ~ 15 nm rms. This would be suitable for glass substrates ($n = 1.5$) at 1.0–2.2 μm as well as silicon substrates ($n = 3.4$) at 2.2–4.8

μm . It should be noted that after coating, the substrate will deform under the stress of the coatings, taking on a concave or convex shape. However, this does not have any effect on the wavefront error in transmission since the surfaces are parallel.

9. *Single-substrate to be used (cemented filters not acceptable).*

Cemented filters are not considered acceptable because of potential large surface deformations when cooled. In cases where a high SR is not needed, cemented filters may be acceptable.

Items 7–9 are the main requirements for filters to be used in adaptive optics. The specified flatness conforms to an SR of 0.985.

10. *Filter to be designed for a tilt of 5° (to suppress ghost images).*

Items 9–10 assume that these filters will be placed at the pupil image within a camera and the filters are tilted to the optical axis by 5° to avoid ghost images in the focal plane. Alternatively, these filters could be designed to be used with no tilt, but with a wedged substrate.

11. *Scratch/Dig: 40/20.*

This item specifies the maximum size of scratches and digs (pits) that are permitted on the surface of the substrate. The specification 40/20, which is acceptable in most ground-based astronomy applications, requires that scratches be no wider than $4\ \mu\text{m}$ and that the pits be no wider than $200\ \mu\text{m}$ in diameter. A technical description of this specification is given by Bennett & Mattsson (1999).

12. *Diameter: 60 mm, or cut to requested size.*

The coating is typically not good near the edge and some of the filter is blocked by the filter mount. Therefore the filter diameter is typically specified to be about 10% larger than the actual size required by the optics.

13. *Maximum thickness: 5 mm, including blocker for InSb detectors.*

Items 12–13 depends on the application. The thickness/diameter ratio must be of a practical value for polishing and mechanical strength and is usually specified to be about 0.1.

14. *No radioactive materials such as thorium to be used (to avoid spurious detector noise spikes).*

3. Filter Fabrication and Filter Profiles

A number of vendors were contacted to solicit bids on the filter production for the consortium of buyers. The vendor selected was OCLI of Santa Rosa, California. This selection was determined both by price of production, ability to meet the specifications, maturity of the production facilities, and willingness to accept individual orders from the consortium. The filters were cut to size by the vendor for each order.

A production run was ordered to accommodate the filter needs of the following observatories and institutions: Anglo-Australian Observatory, California Institute of Technology, Canada-France-Hawaii Telescope, Carnegie Institution, Center for Astrophysics, Cornell University, European Southern Observatory, Gemini Telescopes, Kiso Observatory, Korean Astronomy Observatory, Kyoto University, MPE-Garching, MPI-Heidelberg, NASA Goddard Space Flight Center, NASA Infrared Telescope Facility, National Astronomical Observatory of Japan, National Optical Astronomy Observatories, Nordic Optical Telescope, Ohio State University, Osservatorio Astrofisico di Arcetri, Subaru Telescope, United Kingdom Infrared Telescope, University of California Berkeley, University of California Los Angeles, Univ. of Cambridge, University of Grenoble, Univ. of Hawaii, University of Wyoming, and the William Herschel Telescope.

Figures 1(a)–(g) show the transmission profiles of the filters that were produced. The profiles are shown at 65 K, as obtained by extrapolating the filter shift with temperature from room temperature to 65 K. Figure 2 shows the J , H , K_s , L' , and M' filter profiles superimposed on the atmospheric transmission at Mauna Kea.

4. Photometric properties

Using a modified version of the ATRAN program (Lord 1992), we constructed models of the telluric absorption as a function of air mass to investigate the photometric properties of the new filter set. Absorption spectra covering the range 0.8–5.0 μm were generated for 10 zenith angles between 0° and 70° for each of five values of the precipitable water vapor content (0.5, 1.0, 2.0, 3.0, and 4.0 mm). The zenith angles correspond to a range of air masses between 1.0 and 2.9. The values of the water vapor content span the range typically found on Mauna Kea (see, e.g., Morrison et al. 1973; Warner 1977; Wallace & Livingston 1984). To examine the photometric characteristics down to an air mass of 0.0, we also calculated spectra for five additional air mass values <1.0 (0.05, 0.10, 0.25, 0.50, and 0.75) for each of the water vapor values. These spectra were generated with ATRAN using a model atmosphere in which both the gas and water vapor content were given by the standard model values (appropriate for Mauna Kea at an air mass of 1) scaled by the air mass value. The water content was then scaled by an additional factor given by the ratio of the desired water vapor value to the standard model value computed by ATRAN for the atmosphere above Mauna Kea. All spectra were computed for an altitude of 4158 m (which is the altitude of the NASA Infrared Telescope Facility) and with a resolution of approximately 100,000.

The telluric absorption spectra were then multiplied by a similar resolution model spectrum of Vega obtained from R. Kurucz (2001). For each filter, we computed synthetic magnitudes by multiplying the resulting spectra by the normalized filter transmission curves and integrating over the wavelength range spanned by the filter. Magnitude differences relative to the original model spectrum of Vega were calculated. In Fig. 3 we show the magnitude differences versus air mass for the case of 2.0 mm precipitable water.

For each filter and water vapor value, the run of magnitude differences as a function of air mass was fitted with a least-squares routine with two functional forms: (1) a linear fit between air masses of 1 and 3 and (2) the rational expression given by Young et al. (1994; see their eq. 7) for the entire range of air masses. The latter expression has the form

$$\Delta m = (a + bX + cX^2)/(1 + dX) \quad (1)$$

where a , b , c , and d are fitting constants and X is the air mass. A detailed discussion of this function is given by Young (1989). Both fits are shown in Fig. 3, and the coefficients are given in Tables 2 and 3.

The linear fit simulates the typical photometric reduction technique employed by ground-based observers to obtain the extinction coefficient in magnitude per air mass. The constant term (the intercept of the linear fit) yields the systematic error in the photometric magnitude incurred by adopting this particular functional form of the atmospheric extinction and extrapolating to zero air mass. Inspection of the values given in Table 2 indicates that systematic errors >0.05 mag result from a linear extrapolation for the K' and M' filters for all values of the water vapor. The errors are decreased only slightly if the fit is restricted to the air mass range 1–2.

As can be seen in Fig. 3, equation (1) provides an excellent fit to all the data points. However, the determination of the four coefficients of such a function from actual observations of standard stars is impractical for most observing programs, as a large number of measurements over a range of air masses are required. Even if these observations were carried out, reliable values can be obtained only if measurements in the completely inaccessible air mass range between 0 and 1 were available. The values in Table 3 are presented for comparison to other photometric filters, such as those discussed by Young et al. (1994).

The proposed filters show greatly improved photometric properties over older filter sets. Krisciunas et al. (1987) summarized the average extinction coefficients at Mauna Kea. Comparison of our values given in column 3 of Table 2 with those given in Table I by Krisciunas et al. (1987) reveals that at the typical water vapor of 2–3 mm of precipitable water for Mauna Kea, the reduction in the extinction coefficient is about a factor of 8 at J. In addition, comparison of the values given in column 2 of Table 2 with those given in Table III of Manduca & Bell (1979) shows that the reduction in the error of extrapolation to zero air mass (which they denote as Δ) is about a factor of 9 at J compared to the KPNO winter values.

As was pointed out by Manduca & Bell (1979), the extinction error upon extrapolation to zero air mass does not affect differential photometry, in which one compares observed fluxes of target objects to those of established standard stars. The extinction errors in this case will be absorbed into the photometric zero points. It should be noted, however, that the extinction error may vary with the temperature of the object being observed. This variation leads to a color term in the extinction coefficient. However, as demonstrated by Manduca & Bell, this term is generally small,

amounting to an error of <0.001 mag for most filters. Only the J band filter analyzed by Manduca & Bell exhibited a significant color dependence. Given that the new J filter is less affected by the atmospheric absorption, we expect that the extinction color term for this filter will be as small as those for the other filters.

The extinction errors introduced by adopting a linear fit may, however, affect absolute photometric measurements as, for example, in the establishment of an exo-atmospheric magnitude system. The latter subject has a number of additional complications beyond the scope of the present paper. We simply wish to point out that such a system requires some way to eliminate the extinction error (for example, with narrowband filters; see Young et al. 1994).

5. Summary

A set of $1\text{--}5\ \mu\text{m}$ filters designed for improved photometry and for use with adaptive optics is described. Although the filter profiles are optimized for maximum throughput, they avoid most of the detrimental effects of atmospheric absorption bands. A production run of these filters has been completed. It is our hope that widespread use of these filters will help produce more uniform photometric results, reduce the magnitude of the color transformation among observatories, and reduce the uncertainty in reductions to zero or unit air mass.

We thank E. Atad, J. Elias, S. Leggett, K. Matthews, and especially T. Hawarden for discussions and input on the filter specifications. We also thank S. Lord for providing a modified version of ATRAN that allowed the calculation of the atmospheric transmission between air masses of 0.0 and 1.0. Filter profiles in electronic form may be found at <http://irtf.ifa.hawaii.edu/Facility/nsfcam/history/newfilters.html>. AT acknowledges the support of NASA Contract NASW-5062 and NASA Grant No. NCC5-538. DS acknowledges the support of the Gemini Observatory, which is operated by the Association of Universities for Research in Astronomy, Inc., under a cooperative agreement with the NSF on behalf of the Gemini partnership: the National Science Foundation (United States), the Particle Physics and Astronomy Research Council (United Kingdom), the National Research Council (Canada), CONICYT (Chile), the Australian Research Council (Australia), CNPq (Brazil), and CONICET (Argentina).

REFERENCES

- Bennett, J. M., & Mattsson, L. 1999, *Introduction to Surface Roughness and Scattering* (2d ed., Washington, DC: Opt. Soc. Am.)
- Krisciunas, K., et al. 1987, *PASP*, 99, 887
- Kurucz, R. 2001, <http://kurucz.harvard.edu/stars.html>

- Lord, S. D. 1992, NASA Tech. Mem. 103957
- Manduca, A., & Bell, R. A. 1979, PASP, 91, 848.
- Morrison, D., Murphy, R. E., Cruikshank, D. P., Sinton, W. M., & Martin, T. Z., 1973, PASP, 85, 255
- Schroeder, D.J. 1987, Astronomical Optics (San Diego: Academic Press) 191
- Simons, D., & Tokunaga, A. T. 2001, PASP, in press (Paper I)
- Wallace, L., & Livingston, W. 1984, PASP, 96, 182
- Warner, J. W. 1977, PASP, 89, 724
- Young, A. T. 1989, in Infrared Extinction and Standardization, Lecture Notes in Physics Vol. 341, ed. E. F. Milone (Berlin: Springer), 6
- Young, A.T., Milone, E.F., & Stagg, C.R. 1994, A&AS, 105, 259

Fig. 1(a)–(g). Filter profiles at a temperature of 65 K. These were measured by the vendor at room temperature, then shifted according to the measured change with temperature of a witness sample.

Fig. 2. J, H, K_s, L', M' filter profiles superimposed on the atmospheric transmission at Mauna Kea kindly provided by G. Milone for 1 mm precipitable water vapor and an air mass of 1.0.

Fig. 3. Extinction plot for 2.0 mm precipitable water. The dashed lines are the linear fits to the magnitudes in the air mass range of 1.0–3.0. The solid lines are the fit to equation (1) in the air mass range of 0.0–3.0.

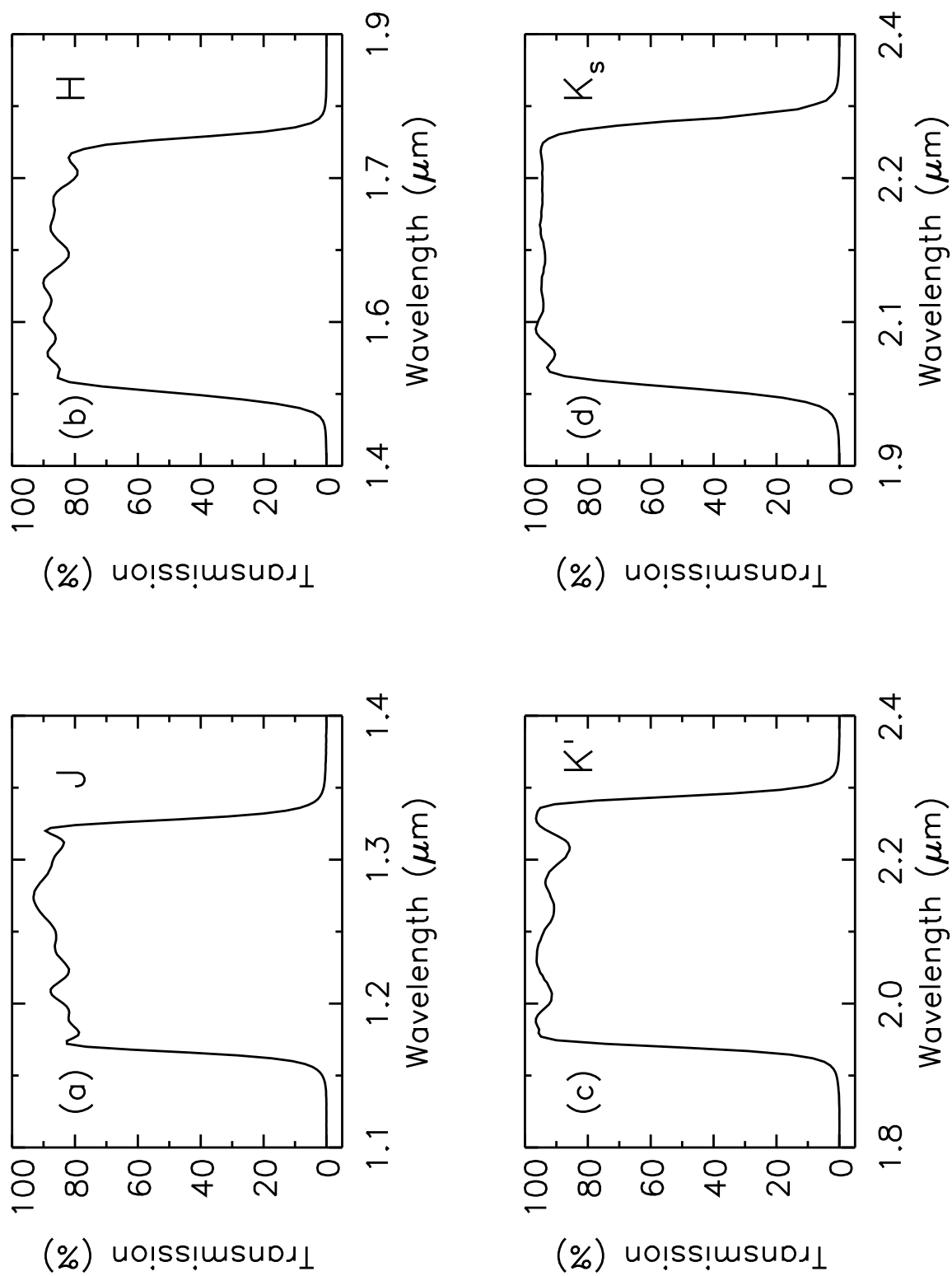


Figure 1(a)–(d)

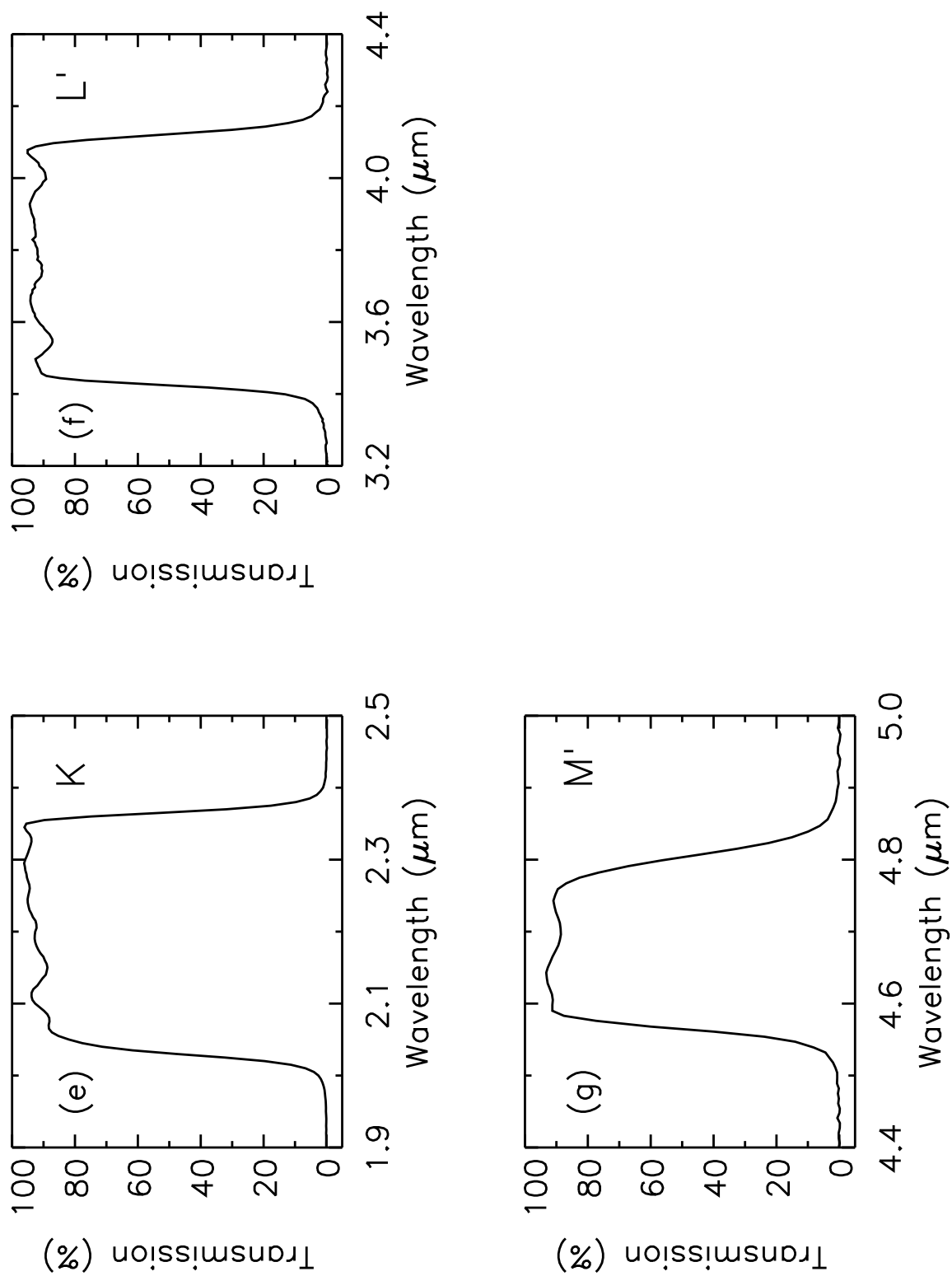


Figure 1(e)–(a)

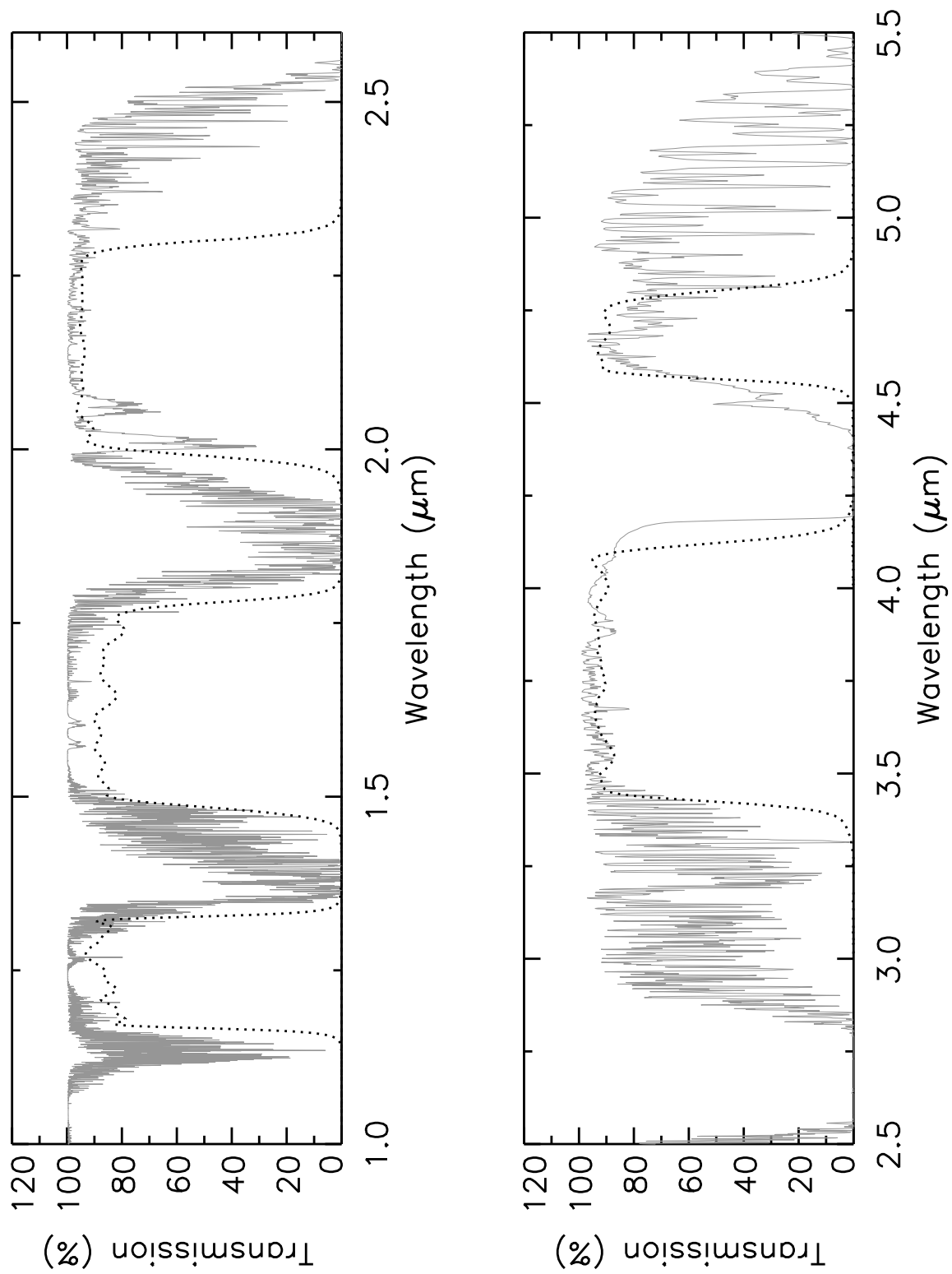


Figure 2

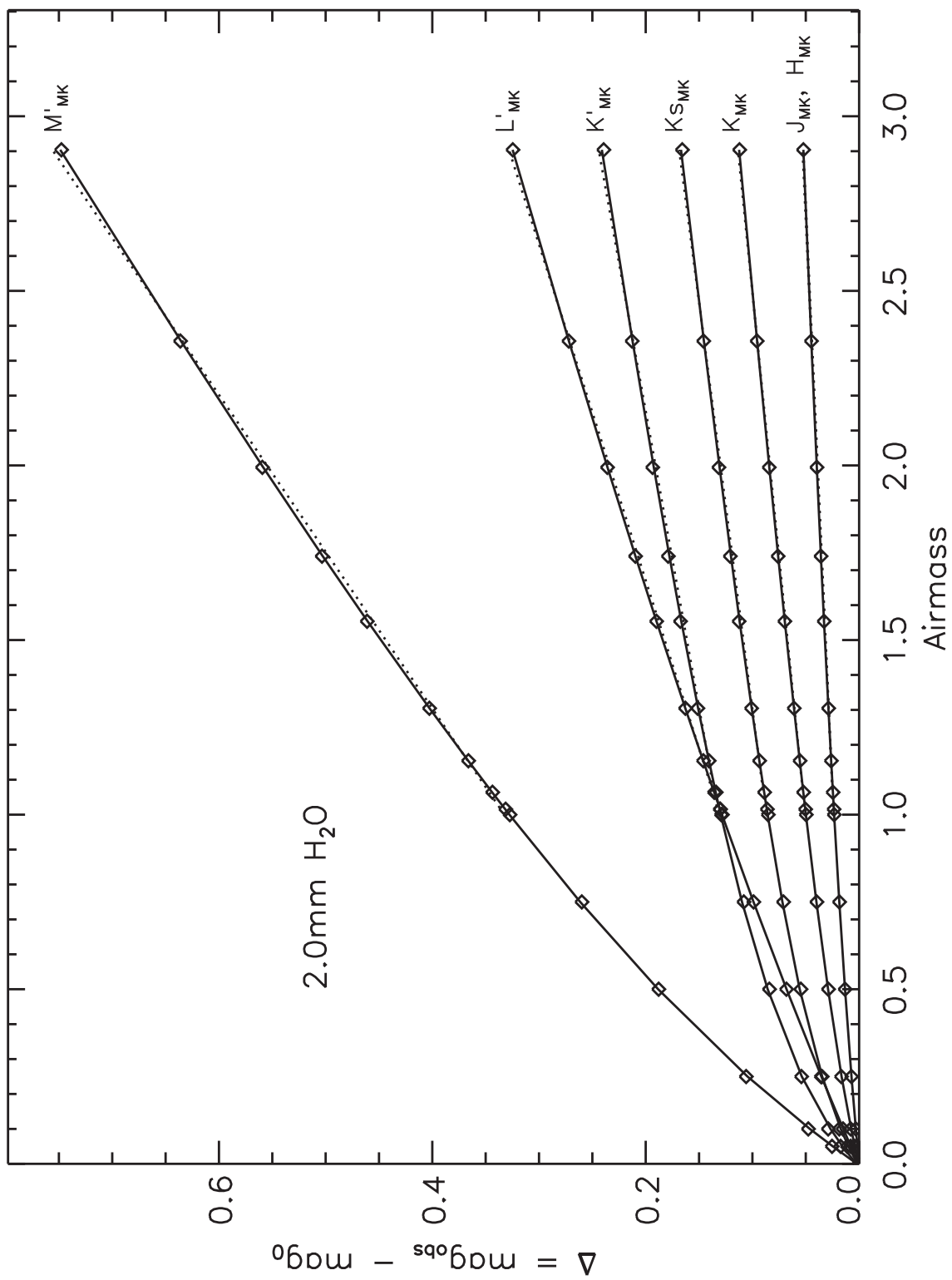


Figure 3

Table 1. Filter Center, Cut-on, and Cut-off Wavelengths

Name	Center	Cut-on	Cut-off
<i>J</i>	1.250	1.170	1.330
<i>H</i>	1.635	1.490	1.780
<i>K'</i>	2.120	1.950	2.290
<i>K_s</i>	2.150	1.990	2.310
<i>K</i>	2.200	2.030	2.370
<i>L'</i>	3.770	3.420	4.120
<i>M'</i>	4.680	4.570	4.790

Note. — The cut-on and cut-off wavelengths correspond to where the transmission is 50% of the peak.

Table 2. Linear Fit to Calculated Extinction Curves

mm H ₂ O/ filter	Constant (mag)	Slope (mag)
0.5 mm		
<i>J</i>	0.0043 ± 0.0002	0.0076 ± 0.0001
<i>H</i>	0.0030 ± 0.0002	0.0088 ± 0.0001
<i>K</i>	0.0170 ± 0.0008	0.0288 ± 0.0004
<i>K'</i>	0.0574 ± 0.0021	0.0491 ± 0.0012
<i>K_s</i>	0.0429 ± 0.0016	0.0384 ± 0.0009
<i>L'</i>	0.0263 ± 0.0019	0.0938 ± 0.0011
<i>M'</i>	0.0956 ± 0.0042	0.2020 ± 0.0025
1.0 mm		
<i>J</i>	0.0056 ± 0.0003	0.0107 ± 0.0002
<i>H</i>	0.0053 ± 0.0003	0.0114 ± 0.0002
<i>K</i>	0.0171 ± 0.0008	0.0304 ± 0.0004
<i>K'</i>	0.0637 ± 0.0023	0.0535 ± 0.0014
<i>K_s</i>	0.0433 ± 0.0016	0.0401 ± 0.0009
<i>L'</i>	0.0261 ± 0.0019	0.0975 ± 0.0011
<i>M'</i>	0.1009 ± 0.0045	0.2109 ± 0.0026
2.0 mm		
<i>J</i>	0.0085 ± 0.0005	0.0153 ± 0.0003
<i>H</i>	0.0091 ± 0.0005	0.0149 ± 0.0003
<i>K</i>	0.0175 ± 0.0008	0.0331 ± 0.0005
<i>K'</i>	0.0731 ± 0.0027	0.0589 ± 0.0015
<i>K_s</i>	0.0442 ± 0.0017	0.0429 ± 0.0010
<i>L'</i>	0.0264 ± 0.0020	0.1039 ± 0.0012
<i>M'</i>	0.1099 ± 0.0049	0.2226 ± 0.0028
3.0 mm		
<i>J</i>	0.0115 ± 0.0006	0.0188 ± 0.0004
<i>H</i>	0.0124 ± 0.0006	0.0173 ± 0.0003
<i>K</i>	0.0180 ± 0.0008	0.0354 ± 0.0005
<i>K'</i>	0.0803 ± 0.0029	0.0625 ± 0.0017
<i>K_s</i>	0.0451 ± 0.0017	0.0452 ± 0.0010
<i>L'</i>	0.0274 ± 0.0021	0.1094 ± 0.0012
<i>M'</i>	0.1170 ± 0.0051	0.2313 ± 0.0030
4.0 mm		
<i>J</i>	0.0144 ± 0.0008	0.0215 ± 0.0004
<i>H</i>	0.0151 ± 0.0007	0.0191 ± 0.0004
<i>K</i>	0.0185 ± 0.0009	0.0375 ± 0.0005
<i>K'</i>	0.0858 ± 0.0030	0.0653 ± 0.0018
<i>K_s</i>	0.0461 ± 0.0017	0.0473 ± 0.0010
<i>L'</i>	0.0288 ± 0.0022	0.1140 ± 0.0013
<i>M'</i>	0.1225 ± 0.0053	0.2380 ± 0.0031

Note. — Least-squares linear fitting to the equation (const. + slope*X), where X is the air mass in the range 1.0–3.0.

Table 3. Fit to Calculated Extinction Curves using Eq. (1)

Filter	a	b	c	d
0.5 mm				
<i>J</i>	0.0000	0.0166	0.0047	0.8166
<i>H</i>	0.0000	0.0146	0.0043	0.6085
<i>K</i>	0.0005	0.0710	0.0301	1.2459
<i>K'</i>	0.0018	0.2376	0.0819	2.0629
<i>K_s</i>	0.0016	0.1782	0.0645	2.0490
<i>L'</i>	0.0006	0.1347	0.0223	0.3311
<i>M'</i>	0.0013	0.4301	0.1953	1.1315
1.0 mm				
<i>J</i>	0.0000	0.0213	0.0050	0.6464
<i>H</i>	0.0001	0.0210	0.0047	0.5642
<i>K</i>	0.0005	0.0718	0.0306	1.1987
<i>K'</i>	0.0022	0.2507	0.0796	1.8836
<i>K_s</i>	0.0016	0.1793	0.0663	2.0116
<i>L'</i>	0.0006	0.1378	0.0228	0.3237
<i>M'</i>	0.0017	0.4402	0.1829	1.0317
2.0 mm				
<i>J</i>	0.0001	0.0310	0.0061	0.5891
<i>H</i>	0.0002	0.0331	0.0082	0.7624
<i>K</i>	0.0006	0.0738	0.0306	1.1041
<i>K'</i>	0.0026	0.2828	0.0851	1.8568
<i>K_s</i>	0.0017	0.1813	0.0680	1.9290
<i>L'</i>	0.0006	0.1441	0.0224	0.2998
<i>M'</i>	0.0020	0.4691	0.1866	1.0066
3.0 mm				
<i>J</i>	0.0001	0.0407	0.0082	0.6464
<i>H</i>	0.0003	0.0449	0.0130	0.9979
<i>K</i>	0.0006	0.0770	0.0322	1.0802
<i>K'</i>	0.0028	0.3163	0.0954	1.9525
<i>K_s</i>	0.0017	0.1851	0.0706	1.8917
<i>L'</i>	0.0006	0.1509	0.0227	0.2908
<i>M'</i>	0.0021	0.5013	0.2067	1.0670
4.0 mm				
<i>J</i>	0.0001	0.0506	0.0113	0.7586
<i>H</i>	0.0003	0.0577	0.0198	1.3120
<i>K</i>	0.0005	0.0807	0.0345	1.0899
<i>K'</i>	0.0028	0.3523	0.1100	2.1260
<i>K_s</i>	0.0017	0.1896	0.0735	1.8790
<i>L'</i>	0.0006	0.1580	0.0244	0.2986
<i>M'</i>	0.0019	0.5381	0.2425	1.1978

Note. — Least-squares fitting to equation (1) in the air mass range of 0.0–3.0.